Chemical Papers (2020) 74:2481–2489
https://doi.org/10.1007/s11696-020-01095-4

ORIGINAL PAPER

Synthesis and characterization of mordenite zeolite from metakaolin and rice husk ash as a source of aluminium and silicon

Marcos Antonio Klunk[1] · Suellen Brasil Schröpfer[1] · Sudipta Dasgupta[2] · Mohuli Das[2] · Nattan Roberto Caetano[3] · Andrea Natale Impiombato[4] · Paulo Roberto Wander[1] · Carlos Alberto Mendes Moraes[1]

Received: 28 November 2019 / Accepted: 6 February 2020 / Published online: 13 February 2020

Abstract
Mordenite zeolite is considered a molecular sieve because of its adsorbent material characteristics used in the industry as a gas separator. High Si/Al ratios of this zeolitic material in its crystal lattice provide high thermal stability in the structure. To minimize the production costs, this work synthesized the mordenite zeolite in absence organic template (high costs of production). For this purpose, rice husk ash (silicon source) was used from a thermoelectric plant that uses biomass for power generation under the "Moving Grade Reactor" method and metakaolin (aluminium source) derived from the construction. To obtain the zeolitic material, an alkaline treatment with sodium hydroxide and deionized water was required. Different Si/Al ratios (5, 10, 15, and 20) were used to evaluate the highest efficiency in adsorption capacity. The textural properties of mordenite as a function of specific surface area ranged from 314 to 347 m^2/g, with micropore volume 0.198–0.279 cm^3/g with average pore diameter ranging from 5.9 to 6.2 Å. N_2 adsorption/desorption isotherms obtained for mordenite presented type IV hysteresis, characteristic of microporous materials. X-ray diffraction showed crystalline phases of mordenite zeolite, mostly. The FTIR reinforces the success of mordenite synthesis by the vibration bands corresponding to the zeolitic material. TGA revealed water desorption and absence of an organic director. The mean cation-exchange capacity values ranged from 1.10 to 1.78 meq/g indicating a 62% increase of 20-mordenite zeolite compared to 5-mordenite in the zeolitization process. This result is satisfactory and promising for the use of mordenite as adsorbent material.

Keywords Biomass · Molecular sieve · Moving grate reactor · Absence organic template

Introduction

Zeolites are hydrated aluminosilicates which have a crystalline structure formed by the combination of silica $(SiO_4)^{4-}$ and alumina $(AlO_4)^{5-}$ tetrahedra joined by oxygen atoms (Klunk et al. 2019a; Lu et al. 2019; Auerbach 2003). For each aluminium atom contained in the structure, an excess negative charge is generated, producing an electrical imbalance (Cherkasov et al. 2016; Matsunaga et al. 2012). Alkali and alkaline Earth act as stabilizers, a striking feature of clay minerals (Klunk et al. 2019b; Elgamouz and Tijani 2018).

The mordenite zeolite (MOR) has 12-ring pores about 6.5 × 7.0 Å in the crystallographic direction of [001] (Ma et al. 2016; Zang et al. 2008; Wahono et al. 2019). They are connected by small pores 8-ring along the direction [010]. MOR belongs to the orthorhombic crystalline system consisting of three mutually perpendicular crystallographic axes with different lengths ($a = 18.1$, $b = 20.5$, and $c = 7.5$ Å). This is an important feature, because the diffusion process is slow compared to the other two- or three-dimensional molecular sieves (13 × and 4A) (Fischer et al. 2018; Garshasbi et al. 2017; Panda and Kumar 2017; Zhou et al. 2015). This behaviour is intensified when the adsorbate molecules are approximately the same size as the pore diameter (Klunk

✉ Marcos Antonio Klunk
marcosak@edu.unisinos.br

[1] Department of Mechanical Engineering, University of Vale do Rio dos Sinos, Av. Unisinos 950, São Leopoldo, RS, Brazil

[2] Indian Institute of Technology Bombay (IIT Bombay), Powai, Mumbai 400076, India

[3] Department of Mechanical Engineering, Federal University of Santa Maria, Av. Roraima 1000, Santa Maria, RS, Brazil

[4] Department of Industrial Engineering, Alma Mater Studiorum University of Bologna, Viale del Risorgimento 2, 40136 Bologna, Italy

et al. 2019c; 2020). As a result, a small fraction of specific molecules can be adsorbed into the cavities of MOR, giving it selectivity, a fundamental feature of molecular sieves (Ma et al. 2016; Nishiyama et al. 1996).

Zeolites can be used for carbon dioxide (CO_2) adsorption to mitigate the environmental impacts caused by greenhouse gas emissions (Santos et al. 2018; Klunk et al. 2019d; Cataluña et al. 2017, 2018; Caetano et al. 2015a). The wide application of zeolites for CO_2 adsorption is enabled due to larger pore cavities compared to the molecular diameter of carbon dioxide (Klunk et al. 2019e; Caetano et al. 2015b, c, 2018). Gas separation in zeolite structure depends on three factors: crystal lattice structure and composition, cationic forms, and zeolite purity (Singh et al. 2018; Hernández-Huesca et al. 1999).

To achieve this purpose, this work aims to synthesize MOR in high purity and crystallinity, in the absence of an organic template. To obtain MOR, rice husk ash (RHA) (silicon source) was used, and for the aluminium source, Metakaolin (MK) ($Al_2O_3.2SiO_2$) was used (Jun Zhang et al. 2018; Zhang et al. 2007). In general, standard synthesis of zeolitic material involves a mineralizing agent (sodium hydroxide) and an organic template (tetrapropylammonium hydroxide) (Hamidzadeh et al. 2018; He et al. 2013; De la Iglesia et al. 2006; Casado 2003). The high cost of manufacturing the zeolitic material is associated with the organic template as they are high-value reagents (Klunk et al. 2019c). Given all these problems, many researchers have sought to develop a methodology for synthesizing MOR in the absence organic template (Radman et al. 2019; Singh et al. 2018; Idris et al. 2018; Zhang et al. 2015; Aly et al. 2012; Huang et al. 2012; Cheng 2008; Kalipçiliar 2007).

To develop efficient adsorbents, MOR was synthesized with different Si/Al ratios (SAR) of 5, 10, 15, and 20. Thus, this work sought to deepen the understanding of the adsorption process and which parameters influence the synthesis of zeolitic material.

Materials and methods

The materials and methodology applied in this work consisted of characterizing the raw materials (RHA and MK) as well as the zeolitic material formed.

Synthesis of mordenite

Mordenite synthesis in absence organic template was performed according to Costa and Araujo (2010) with some modifications. For this purpose, RHA (silicon source) from a thermoelectric power plant located in the state of Rio Grande do Sul-Brazil was used. This company uses biomass for power generation under the method "Moving Grade Reactor" (Fernandes et al. 2016, 2017a, 2018; Moraes et al. 2014). Therefore, MK ($Al_2O_3.2SiO_2$) was used as an aluminium source. This feedstock is related to the passage from the hydrated state of kaolin ($Al_2O_3.2SiO_2.2H_2O$) to dehydrate through dehydroxylation of the kaolinite molecule ($Al_2Si_2O_5(OH)_4$) through calcination at controlled temperatures (Gardolinski et al. 2003).

The contribution of metakaolin plays an important role in the adjustment of the effective charges in the crystal lattice of the zeolitic material. According to Table 1, we can identify that the major compounds are SiO_2 and Al_2O_3. Unlike RHA, which has 90% SiO_2, metakaolin enters the mordenite synthesis not to aggregate SiO_2 to the structure, but to compensate for the alumina $(AlO_4)^{5-}$ deficit in the molecular sieve tetrahedral lamellae. Another important point of MK is the contribution of SiO_2 in zeolite formation, even if less significant compared to Al_2O_3.

The characteristics of the two raw materials, precursors of the zeolitic material, are shown in Table 1. Potential applications of RHA and MK were defined by the chemical composition, which was determined by X-ray fluorescence. The present compounds are derived from the inorganic fraction present in RHA and MK, so the results are presented as more stable binary oxides (Fernandes et al. 2017b).

The synthesis methodology consists of reactions under alkaline conditions (NaOH—3.5 mol/L). The reaction system is divided into two equal parts of the same volume (500 mL of NaOH). The first part is used to dissolve the RHA and the second part to dissolve the MK according to the mass in grams of each raw material to obtain the Si/Al ratios (Table 2). The two solutions were then carefully mixed and left at room temperature to allow the transformation of the sol–gel process. The gel was then oven-dried at 90 °C for 24 h. The dried solid was ground and subsequently calcined at 550 °C for 6 h.

Characterization of materials

The characterization of the zeolitic material is fundamental for understanding the adsorption process. Thus, the techniques used in this work are: (1) specific surface area (BET),

Table 1 Chemical analysis of the compounds present in the RHA (Fernandes et al. 2016) and MK (wt%) by XRF

Composition	RHA	MK
SiO_2	90.02	48.27
Al_2O_3	0.08	35.34
Fe_2O_3	0.01	1.08
K_2O	0.81	2.62
CaO	ND	3.80
MgO	ND	2.97
TiO_2	ND	3.58
SO_3	0.07	ND

Table 2 Quantities of raw material and molar composition used for the synthesis of mordenite in absence organic template for the different Si/Al ratios

SAR	RHA (g)	MK (g)	Molar composition
5	3.85	7.80	$0.23SiO_2$:$0.12Al_2O_3$:11.19NaOH:27.$78H_2O$
10	4.52	9.14	$0.27SiO_2$:$0.15Al_2O_3$:11.19NaOH:27.$78H_2O$
15	5.73	11.59	$0.34SiO_2$:$0.18Al_2O_3$:11.19NaOH:27.$78H_2O$
20	6.81	13.88	$0.41SiO_2$:$0.22Al_2O_3$:11.19NaOH:27.$78H_2O$

(2) chemical composition (XRF), (3) mineral composition (XRD), (4) identification of specific functional groups (FTIR), (5) SEM/EDS was utilized in the present work to complement the other characterization techniques, (6) thermal analysis in which the variation of sample mass (loss or gain) is determined as a function of temperature and/or time (TGA), and (7) cation-exchange capacity (CEC). To evaluate CEC, the methodology of Shinzato et al. 2008 with some modifications was applied.

The cation-exchange capacity (CEC) was performed as follows:

(1) 1.0 g of sample with 100 mL of one molar sodium acetate solution ($CH_3COONa.3H_2O$).
(2) Stirring at room temperature for 24 h at 120 rpm.
(3) Filter the sample, and the analyte retained on the filter, should be washed with 1.0 L of deionized water, and oven-dried at 80 °C for 2 h.
(4) In the dry sample, stir at room temperature for 24 h at 120 rpm with 100 mL of one molar ammonium acetate solution (CH_3COONH_4).
(5) Filter the suspension and the Na^+ ions and concentration determined by the inductively coupled plasma optical emission spectrometry (ICP-OES) technique. The amount of sodium ion was expressed in mg/L (ppm) and converted to the usual milli-equivalent of CEC units (meq/g).

Results and discussion

Characterization of mordenite

Table 3 shows the amounts in grams of unreacted material after alkaline treatment as well as the yield of mordenite synthesis.

We can observe that for all samples, the reaction system yield is above 70%. The residues found in the reactions come from the sol–gel system filtration step. The remaining (unreacted) precursor materials composed of SiO_2 (RHA) and $Al_2O_3.2SiO_2.2H_2O$ (MK) obstruct the filtration system making it difficult to separate sol–gel.

Table 3 Gel quantity and leftover grams of Si and Al forming impurities as well as the yield of the reactions

SAR	Gel composition (g)	Residues of Si/Al (g)	Yield (%)
5	11.66	3.14	73
10	13.74	4.09	70
15	17.33	5.02	71
20	20.70	5.59	73

Measurements of the surface area (BET), volume, and average pore diameter of the zeolitic material are listed in Table 4. For low and intermediate silicon ratios, between 5 and 10, the BET ranged from 314 to 328 m^2/g, with an average pore diameter of 5.9 Å. Therefore, for high Si/Al ratios, between 15 and 20, the surface area is in the range of 339–347 and an average pore diameter between 6.0 and 6.2 Å. The BET results found in this study are in agreement with the works of Zhang et al. (2011), Mignoni et al. (2007), Dimitrova et al. (2006), and Hincapie et al. (2004) that use the synthesis of mordenite by the traditional method.

Synthesized mordenite has, in all Si/Al ratios, pore volume identified in the micro-range (less than 2 nm) according to Meier and Olson (1992).

Increased SAR results in an 11% increase in surface area (Table 4). This increase is related to the formation of a crystal lattice made up of Si and Al tetrahedra. The results indicated that as Si and Al are incorporated into the crystal lattice, the micropore volume of mordenite increases, which leads to a larger pore volume. Another factor contributing to the increase in surface area is the fact that adsorption of nitrogen molecules does not occur uniformly in a monolayer, but in the form of irregular layers, where the monolayer is often not fully filled until another layer begins to

Table 4 Textural properties of mordenite zeolites in different SARs

SAR	BET surface area (m^2/g)	Pore volume (cm^3/g)		Average pore diameter (Å)
		Micropore (*t* plot)*	Mesopore (BJH)**	
5-MOR	314	0.198	0.01	5.9
10-MOR	328	0.237	0.02	5.9
15-MOR	339	0.252	0.02	6.0
20-MOR	347	0.279	0.03	6.2

*Used to determine the microporous volumes in porous materials including hierarchical zeolites

**Barett–Joyner–Halenda method (method to calculate the mesopore-size distribution from adsorption isotherm data)

form, which, consequently, changes the value of the specific surface area.

After obtaining the zeolitic material, the micropore volume has increased from 0.198 to 0.279 cm^3/g. The size of the adsorbed molecules plays an important role in their adsorption on zeolite. Zeolite cavities are a selective factor for adsorbed molecules. Mordenite can adsorb molecules that have a maximum diameter of 0.4 nm, indicating that CO_2 adsorption (diameter = 0.33 nm) is not limited by this steric factor (Bonenfant et al. 2008; Aguilar-Armenta et al. 2001; Hernández-Huesca et al. 1999). In addition, the time required to reach the middle CO_2 adsorption capacity is proportional to the diameter of the adsorbed molecules (Dunne et al. 1996; Hayhurst 1980). This behaviour is similar when other forms of adsorbents such as non-mineralizable coals are used (Klunk et al. 2018). Figure 1 shows the nitrogen adsorption–desorption isotherms for mordenite zeolite samples in the different SARs. The results indicate a slight increase in relative pressure (p/p_0) in the ranges of 0.01 and 0.97.

For low relative pressure, this behaviour can be interpreted by the fact that zeolites are filling the micropores of their structure, which means the presence of microporous cavities. Therefore, for high pressures, rapid absorption occurs indicating the existence of empty cavities resulting from the crystalline structure of the zeolitic material. In addition, the formed zeolites show a hysteresis loop at relative pressures (p/p_0) between 0.42 and 0.96 caused by mesoporous channels. The obtained isotherms demonstrated that all samples exhibit the typical type IV adsorption isotherm with the H3 hysteresis loop, as identified by the IUPAC.

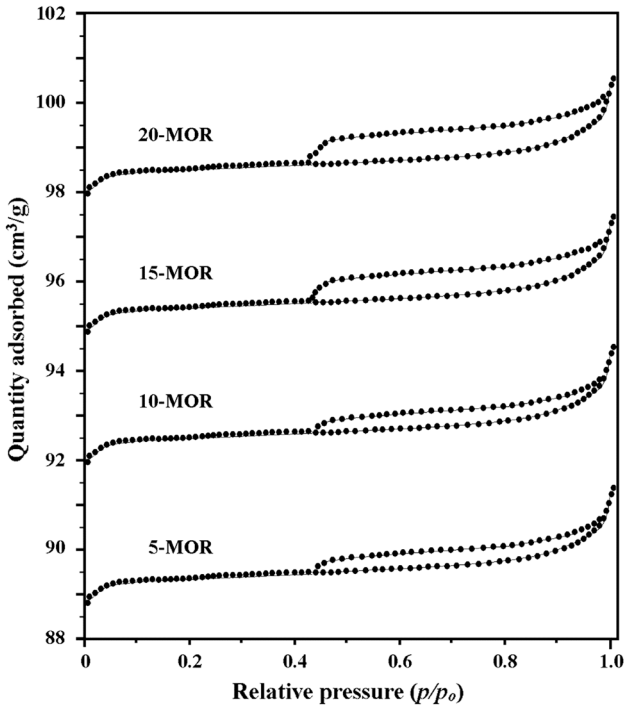

Fig. 1 N_2 adsorption and desorption isotherms of mordenite

According to Table 5, there was a wide variation between the contents of the main components present in zeolites formed with different SARs.

For 5-MOR zeolite, X-ray fluorescence reveals that SAR is 4.64. In sample 10-MOR, the Si/Al ratio is 10.32. Thus, in zeolitic materials 15-MOR and 20-MOR, the SAR are 15.47 and 21.96, respectively. Due to experimental errors, reagent impurity, and instrumental inaccuracy, the exact SARs of 5, 10, 15, and 20 could not be obtained by synthesis. The zeolites formed presented, in general, high contents of silica, alumina, ferric oxide, and sodium oxide that favour the formation of mordenite. Calcium oxide, titanium, magnesium, sulfur, potassium, and other compounds were also found in amounts of less than 5%.

The low sulfur content and high amounts of calcium enhance the use of these materials. Sodium content is related to its incorporation into the zeolitic material by hydrothermal synthesis, where metakaolin was used as an external aluminium source and activating agent, respectively. Exposure of the material to solutions with higher NaOH concentrations during synthesis increased the amount of sodium in the zeolite structure (Scott et al. 2001).

To identify the formation of the crystal structure of MOR in the absence of organic template, they were submitted to XRD analysis. The diffractograms obtained are shown in Fig. 2. The results of XRD were based on the International Union Database Database's Joint Committee on Powder Diffraction Standards (JCPDS) (Scapin 2003; Atkins and Jones 2001). The peaks between 2θ of 5° and 30° correspond to mordenite in all SARs. Thus, mordenite is favoured by the addition of metakaolin due to the high amounts of calcium and potassium elements that are part of its crystal

Table 5 Chemical analysis of the compounds present in the MOR (% by mass)

Oxides	5-MOR	10-MOR	15-MOR	20-MOR
SiO_2	59.41	61.08	62.95	65.67
Al_2O_3	12.8	5.92	4.07	2.99
Fe_2O_3	3.53	3.92	4.95	4.88
Na_2O	0.54	0.59	0.66	0.80
K_2O	5.81	5.91	6.60	6.78
CaO	1.52	1.66	1.70	2.07
MgO	0.79	0.80	0.91	0.88
TiO_2	4.88	4.51	3.80	3.00
SO_3	0.08	0.07	0.06	0.01
SiO_2/Al_2O_3	4.64	10.32	15.47	21.96

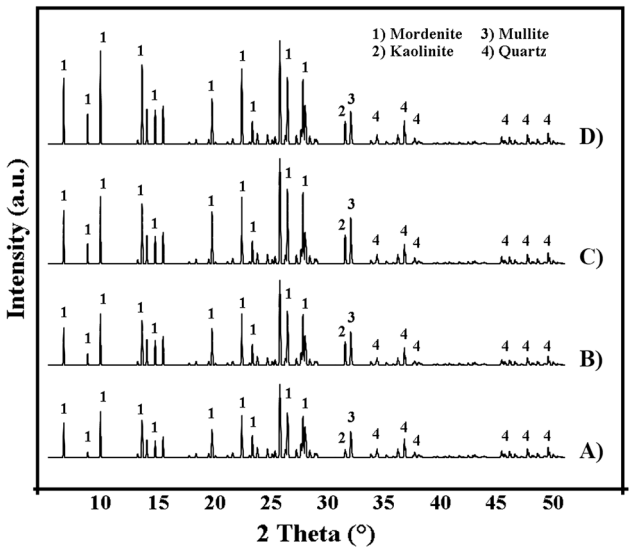

Fig. 2 Diffractogram of mordenite zeolites with different Si/Al ratios: **a** 5, **b** 10, **c** 15, and **d** 20

lattice. The chemical formulas of the crystalline phases of the zeolitic material are shown in Table 6.

The diffractograms reveal the formation of kaolinite, mullite, and quartz between 2θ of 31° and 50° (peaks with low intensity). These results are in accordance with research conducted by Mignoni et al. (2007) and Shao et al. (2001) who synthesized mordenite with external sources of aluminium. The occurrence of kaolinite and mullite is related to the reactions that occur between SiO_2 (RHA) and $Al_2O_3.2SiO_2$ (metakaolin).

In general, quartz cannot be dissolved by hydrothermal processes and remain in the zeolitic material. These compounds were found in varying amounts in all samples. Aluminium is an element that constitutes the crystalline network of zeolites, and therefore, its quantities directly influence the formation of adsorbents. It is noteworthy that the identification of the crystalline phases in the samples with the addition of metakaolin served to obtain the various Si/Al ratios.

The results, compared with literature data, prove that the molar ratios used and the synthesis conditions favour the formation of the zeolitic material (Hisham et al. 2012; Xianfeng et al. 2009; Zhang et a. 2002).

Table 6 Crystalline structures and chemical formula of zeolitic compounds

Crystalline structures	Chemical formula
Quartz	SiO_2
Mordenite	$(Ca,Na_2,K_2)Al_2Si_{10}O_{24}\bullet 7(H_2O)$
Mullite	$Al_{4,44}Si_{1,56}O_{9,78}$
Kaolinite	$Al_2Si_2O_5(OH)_4$

Fourier transform infrared spectroscopy (FTIR) of the 5-MOR, 10-MOR, 15-MOR, and 20-MOR samples are in Fig. 3. All samples exhibit the same profile in the FTIR spectra. In this way, the samples reveal typical mordenite vibrational bands (Ivanova and Knyazeva 2013).

The mordenite FTIR spectra exhibit two vibrational peaks of 3744 cm^{-1} and 3605 cm^{-1} associated with the silanol end-groups (Si–O–H and Si–OH–Al). In addition, the band observed around 3655 cm^{-1} corresponds to aluminium vibrations (AlOH–). The H–OH flexion bands were observed at 1636 cm^{-1} and 1230 cm^{-1}, and are attributed to the –OH vibration. Vibrational stretches were found at 1040 cm^{-1} related to the Si–O group.

The wavelengths of 800 cm^{-1}, 550 cm^{-1}, and 468 cm^{-1} are related to the vibrations of Al–O–Al, Si–O–Si, and internal asymmetric stretching of Al–O and Si–O (Bevilacqua and Busca 2002).

Fig. 4a and b shows the SEM/EDS demonstrations from mordenite zeolite (sample 20-MOR). This sample

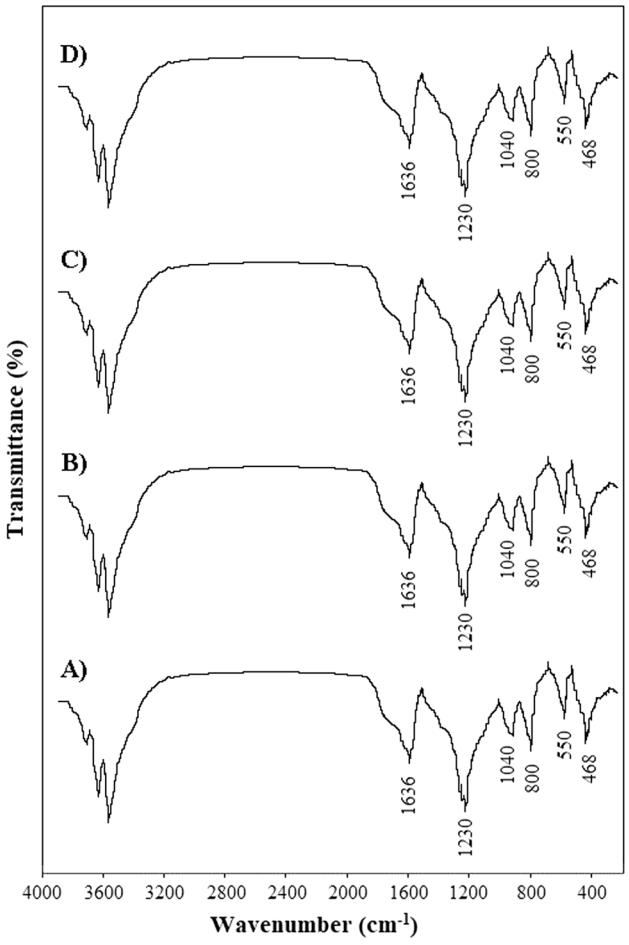

Fig. 3 Infrared spectrum for mordenite zeolites without different Si/Al ratios and without the use of organic guidance: **a** 5-MOR, **b** 10-MOR, **c** 15-MOR, and **d** 20-MOR

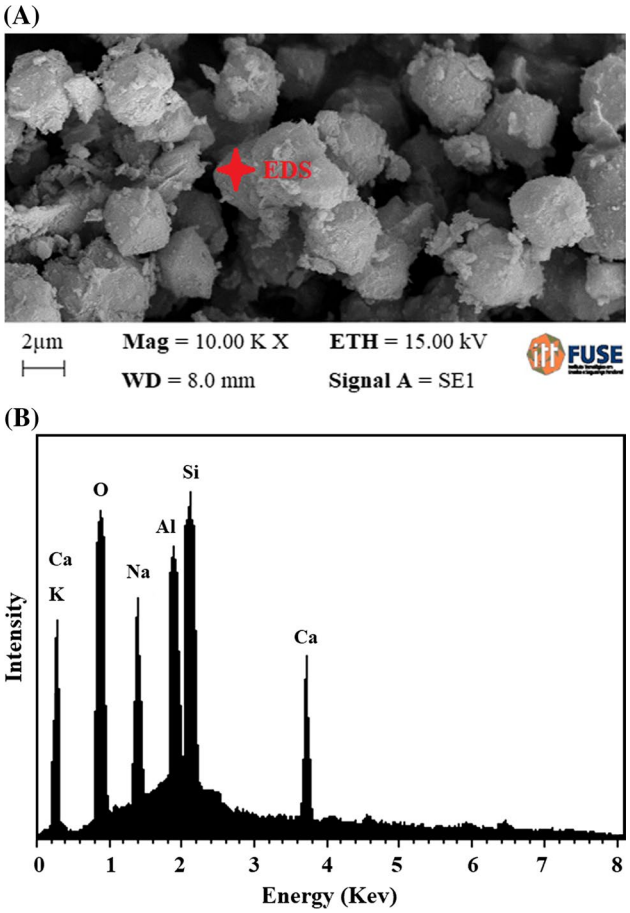

Fig. 4 Scanning electron micrographs (**a**) and energy-dispersive spectroscopy (**b**) of mordenite zeolites formed from RHA and MK

has a typical appearance characterized by the presence of irregular-shaped angular particles (RHA burning takes place in the pulverized form) of varying sizes (Fig. 4a). The combustion conditions of RHAs in the thermoelectric power plants determine the morphology of the particles.

According to the EDS technique, the presence of the chemical elements Ca, Na, K, Al, Si, and O_2 acts as evidence for the formation of zeolite called mordenite.

Thermogravimetric tests were performed to identify the mass loss regions for the zeolitic material formed. Thermogravimetric curves are shown in Fig. 5. These curves show a region of marked mass loss from 100 °C to approximately 300 °C. This loss comprises the desorption of water not bound to the structure and because they do not have organic material. The samples obtained in the absence of organic template had two less mass loss steps when compared to the studies by Frantz (2015), Costa (2013), and Caldeira (2011) that used organic template. Mass loss is higher for samples with lower Si/Al ratio. However, all samples stabilize mass losses around 400 °C.

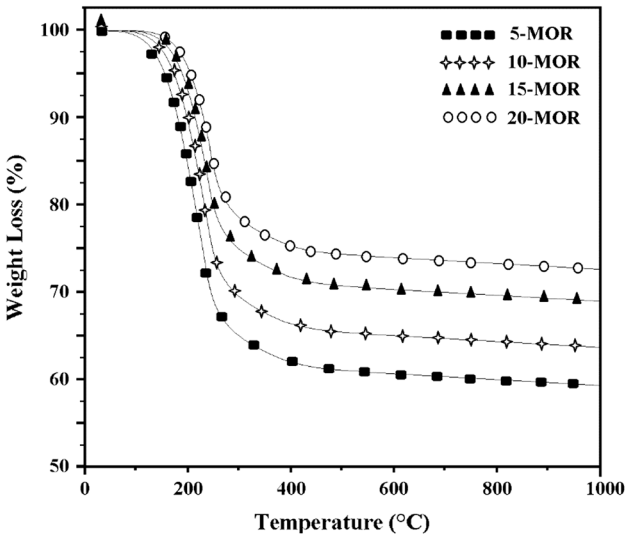

Fig. 5 TGA plots of mordenite in SAR 5, 10, 15, and 20 in absence of organic template

The results of the cation-exchange capacity measurements using ICP-OES of the zeolitic material are shown in Table 7.

Mean CEC values ranged from 1.10 to 1.78 meq/g. There was a 62% increase in CEC of 20-MOR zeolite compared to 5-MOR in the zeolitization process. This was due to the high surface area (about 11% greater than 5-MOR compared to 20-MOR) associated with the micropore volume which increased 41%. 20-MOR zeolites are easier to exchange NH_4^+ when compared to 5-MOR. The CEC values found for all MOR zeolites, synthesized without an organic director, indicate that these materials have a high potential for use as ion exchangers.

Table 7 CEC for mordenite zeolites according to Si/Al ratio

Zeolite MOR	CEC (meq/g)	Average
5	1.10	1.10
	1.09	
	1.10	
10	1.36	1.36
	1.36	
	1.36	
15	1.57	1.57
	1.57	
	1.57	
20	1.80	1.78
	1.77	
	1.77	

Conclusions

Synthesized mordenite from external sources of Si (RHA) and Al (MK) in absence organic template resulted in a high crystallinity zeolitic material, proven by XRD with 70% of the yield. Zeolite characterization revealed an 11% increase in surface area when compared to 5-MOR with 20-MOR. As a consequence, the N_2 adsorption/desorption isotherms obtained for mordenite presented type IV adsorption isotherm with the H3 hysteresis loop of microporous materials. The hysteresis curves revealed that they can be reused without loss in adsorption capacity. The chemical composition of Si/Al ratios in the formed zeolites 5-MOR (4.64), 10-MOR (10.32), 15-MOR (15.47), and 20-MOR (21.96) proved the success of the synthesis. These transformations were due to the efficient alkaline treatment that provided the formation of zeolitic material. Fourier transform infrared spectroscopy reinforces the success of mordenite synthesis by the vibration bands corresponding to Al–O–Al and Si–O–Si stretches, and coupling vibration Al–O and Si–O typical of zeolitic material. The SEM demonstrations in the presence of irregular-shaped angular particles from RHA burning takes place in the pulverized form), and according to EDS technique, the presence of the chemical elements Ca, Na, K, Al, Si, and O_2 acts as evidence for the formation of zeolite called mordenite. The results of thermogravimetric tests reveal water desorption and absence of organic director with high mass loss in the range of 100–300 °C, acquiring stability after 400 °C. Thus, it can be concluded that the higher the Si/Al ratio in the samples, the higher the thermal stability. The 20-MOR cation-exchange capacity was 62% higher compared to the low Si/Al ratio. This result is satisfactory and promising for the use of MOR as adsorbent material.

Acknowledgements The authors acknowledge the Brazilian agencies CNPq (National Council of Technological and Scientific Development—Brasília, DF, Brazil), CAPES (Coordination for the Improvement of Higher Education Personnel) for the research funding and research grants for some of the authors (PNPD/CAPES and DT2/CNPq), and the generous assistance of all the people from the company who granted us access to their database and perception information.

References

Aguilar-Armenta G, Hernandez-Ramirez G, Flores-Loyola E, Ugarte-Castaneda A, Silva-Gonzalez R, Tabares-Munoz C, Jimenez-Lopez A, Rodriguez-Castellon E (2001) Adsorption kinetics of CO_2, O_2, N_2, and CH_4 in cation-exchanged clinoptilolite. J Phys Chem B 105(7):1313–1319. https://doi.org/10.1021/jp9934331

Aly HM, Moustafa ME, Abdelrahman EA (2012) Synthesis of mordenite zeolite in absence of organic template. Adv Powder Technol 23(6):757–760. https://doi.org/10.1016/j.apt.2011.10.003

Atkins P, Jones L (2001) Princípios de Química—questionando a vida moderna e o meio ambiente. Bookman, Porto Alegre

Auerbach S (2003) Handbook of zeolite science and technology. CRC Press, Boca Raton

Bevilacqua M, Busca G (2002) A study of the localization and accessibility of Brønsted and Lewis acid sites of H-mordenite through the FTIR spectroscopy of adsorbed branched nitriles. Catal Commun 3:497–502. https://doi.org/10.1016/S1566-7367(02)00196-6

Bonenfant D, Kharoune M, Niquette P, Mimeault M, Hausler R (2008) Advances in principal factors influencing carbon dioxide adsorption on zeolites. Sci Technol Adv Mater 9(1):013007. https://doi.org/10.1088/1468-6996/9/1/013007

Caetano NR, Cataluña R, Vielmo HA (2015a) Analysis of the effect on the mechanical injection engine using doped diesel fuel by ethanol and bio-oil. Int Rev Mech Eng 9(2):124–128. https://doi.org/10.15866/ireme.v9i2.4341

Caetano NR, Soares D, Nunes RP, Pereira FM, Schneider PS, Vielmo HA, van der Laan FT (2015b) A comparison of experimental results of soot production in laminar premixed flames. Open Eng 5:213–219. https://doi.org/10.1515/eng-2015-0016

Caetano NR, Stapasolla TZ, Peng FB, Schneider PS, Pereira FM, Vielmo HA (2015c) Diffusion flame stability of low calorific fuels. Defect Diffus Forum 362:29–37. https://doi.org/10.4028/www.scientific.net/DDF.362.29

Caetano NR, Venturini MS, Centeno FR, Lemmertz CK, Kyprianidis KG (2018) Assessment of mathematical models for prediction of thermal radiation heat loss from laminar and turbulent jet non-premixed flames. Therm Sci Eng Prog 7:241–247. https://doi.org/10.1016/j.tsep.2018.06.008

Caldeira VPDS (2011) Avaliação da síntese e caracterização de zeólita ZSM-5 ausente de direcionador orgânico estrutural. Dissertação, Universidade Federal do Rio Grande do Norte

Casado L (2003) Preparation, characterization and pervaporation performance of mordenite membranes. J Membr Sci 216(1–2):135–147. https://doi.org/10.1016/s0376-7388(03)00065-6

Cataluña R, Shah Z, Pelisson L, Caetano NR, Da Silva R, Azevedo C (2017) Biodiesel glycerides from the soybean ethylic route incomplete conversion on the diesel engines combustion process. J Braz Chem Soc. https://doi.org/10.21577/0103-5053.20170100

Cataluña R, Shah Z, Venturi V, Caetano NR, Da Silva BP, Azevedo CMN, Da Silva R, Suarez PAZ, Oliveira LP (2018) Production process of di-amyl ether and its use as an additive in the formulation of aviation fuels. Fuel 228:226–233. https://doi.org/10.1016/j.fuel.2018.04.167

Cheng Y, Liao RH, Li JS, Sun XY, Wang LJ (2008) Synthesis research of nanosized ZSM-5 zeolites in the absence of organic template. J Mater Process Technol 206(1–3):445–452. https://doi.org/10.1016/j.jmatprotec.2007.12.054

Cherkasov N, Vazhnova T, Lukyanov DB (2016) Quantitative infra-red studies of Brønsted acid sites in zeolites: case study of the zeolite mordenite. Vib Spectrosc 83:170–179. https://doi.org/10.1016/j.vibspec.2016.02.002

Costa MJF (2013) Síntese de catalisadores nanoporosos na ausência total e parcial de direcionadores orgânicos para pirólise catalítica de óleos pesados e intermediários. 2013. Tese Universidade Federal do Rio Grande do Norte, Natal.

Costa MJF, Araujo AS (2010) Zeólitas Sintetizadas na Ausência Total de Direcionador Orgânico e Respectivo Processo de Síntese. Rev Propr Ind 2083:76–76

De la Iglesia Ó, Irusta S, Mallada R, Menéndez M, Coronas J, Santamaría J (2006) Preparation and characterization of two-layered mordenite-ZSM-5 bi-functional membranes. Microporous Mesoporous Mater 93(1–3):318–324. https://doi.org/10.1016/j.micromeso.2006.03.012

Dimitrova R, Gündüz G, Spassova M (2006) A comparative study on the structural and catalytic properties of zeolites type ZSM-5,

mordenite, beta and MCM-41. J Mol Catal A Chem 243(1):17–23. https://doi.org/10.1016/j.molcata.2005.08.015

Dunne JA, Rao M, Sircar S, Gorte RJ, Myers AL (1996) Calorimetric heats of adsorption and adsorption isotherms. 2. O_2, N_2, Ar, CO_2, CH_4, C_2H_6, and SF_6 on NaX, H-ZSM-5, and Na-ZSM-5 zeolites. Langmuir 12(24):5896–5904. https://doi.org/10.1021/la960496r

Elgamouz A, Tijani N (2018) Dataset in the production of composite clay-zeolite membranes made from naturally occurring clay minerals. Data Brief 19:2267–2278. https://doi.org/10.1016/j.dib.2018.06.117

Fernandes IJ, Calheiro D, Kieling AG, Moraes CAM, Rocha TLAC, Brehm FA, Modolo RCE (2016) Characterization of rice husk ash produced using different biomass combustion techniques for energy. Fuel 165:351–359. https://doi.org/10.1016/j.fuel.2015.10.086

Fernandes IJ, Calheiro D, Sánchez FAL, Camacho ALD, Rocha TLAC, Moraes CAM, Sousa VC (2017a) Characterization of silica produced from rice husk ash: comparison of purification and processing methods. Mater Res 20:512–518. https://doi.org/10.1590/1980-5373-mr-2016-1043

Fernandes IJ, Sánchez FAL, Jurado JR, Kieling AG, Rocha TLAC, Moraes CAM, Sousa VC (2017b) Physical, chemical and electric characterization of thermally treated rice husk ash and its potential application as ceramic raw material. Adv Powder Technol 28(4):1228–1236. https://doi.org/10.1016/j.apt.2017.02.009

Fernandes IJ, Santos RV, dos Santos ECA, Rocha TLAC, Domingues Junior NS, Moraes CAM (2018) Replacement of commercial silica by rice husk ash in epoxy composites: a comparative analysis. Mater Res 21(3):1–10. https://doi.org/10.1590/1980-5373-mr-2016-0562

Fischer F, Lutz W, Buhl J-C, Laevemann E (2018) Insights into the hydrothermal stability of zeolite 13X. Microporous Mesoporous Mater 262:258–268. https://doi.org/10.1016/j.micromeso.2017.11.053

Frantz TS (2015) Síntese e caracterização de zeólitas do tipo ZSM-5 para a adsorção de CO_2. Dissertação, Universidade Federal do Rio Grande, Rio Grande

Gardolinski JE, Martins Filho HP, Wypych F (2003) Thermal behavior of hydrated kaolinite. Quim Nova 26(1):30–35. https://doi.org/10.1590/S0100-40422003000100007

Garshasbi V, Jahangiri M, Anbia M (2017) Equilibrium CO_2 adsorption on zeolite 13X prepared from natural clays. Appl Surf Sci 393:225–233. https://doi.org/10.1016/j.apsusc.2016.09.161

Hamidzadeh M, Komeil S, Saeidi M (2018) Seed-induced synthesis of ZSM-5 aggregates using the silicate-1 as a seed: characterization and effect of the silicate-1 composition. Microporous Mesoporous Mater 268:153–161. https://doi.org/10.1016/j.micromeso.2018.04.016

Hayhurst DT (1980) Gas adsorption by some natural zeolites. Chem Eng Commun 4(6):729–735. https://doi.org/10.1080/00986448008935944

He Y, Liu M, Dai C, Xu S, Wei Y, Liu Z, Guo X (2013) Modification of nanocrystalline HZSM-5 zeolite with tetrapropylammonium hydroxide and its catalytic performance in methanol to gasoline reaction. Chin J Catal 34(6):1148–1158. https://doi.org/10.1016/s1872-2067(12)60579-8

Hernández-Huesca R, Diaz L, Aguilar-Armenta G (1999) Adsorption equilibria and kinetics of CO_2, CH_4 and N_2 in natural zeolites. Sep Purif Technol 15(2):163–173. https://doi.org/10.1016/s1383-5866(98)00094-x

Hincapie BO, Garces LJ, Zhang Q, Sacco A, Suib SL (2004) Synthesis of mordenite nanocrystals. Microporous Mesoporous Mater 67(1):19–26. https://doi.org/10.1016/j.micromeso.2003.09.026

Hisham MA, Moustafa EM, Ehab AA (2012) Synthesis of mordenite zeolite in absence of organic template. Adv Powder Technol 23:757–760. https://doi.org/10.1016/j.apt.2011.10.003

Huang X, Zhang R, Wang Z (2012) Controlling crystal transformation between zeolite ZSM-5 and mordenite without organic structure-directing agent. Chin J Catal 33(7–8):1290–1298. https://doi.org/10.1016/s1872-2067(11)60400-2

Idris A, Khalil U, AbdulAziz I, Makertihartha IGBN, Subagjo Laniwati M, Muraza O (2018) Fabrication zone of OSDA-free and seed-free mordenite crystals. Powder Technol 342:992–997. https://doi.org/10.1016/j.powtec.2018.09.041

Ivanova II, Knyazeva EE (2013) Micro–mesoporous materials obtained by zeoliterecrystallization: synthesis, characterization and catalytic applications. Chem Soc Rev 42(9):3671–3688. https://doi.org/10.1039/c2cs35341e

Jun Zhang Y, Chen H, Yang He P, Juan Li C (2018) Developing silica fume-based self-supported ECR-1 zeolite membrane for seawater desalination. Mater Lett. https://doi.org/10.1016/j.matlet.2018.10.167

Kalipçilar H, Çulfaz A (2007) Template-free synthesis of ZSM-5 type zeolite layers on porous alumina disks. Turk J Chem 31:233–242

Klunk MA, Dasgupta S, Das M, Shah Z (2018) System of adsorption of CO_2 in coalbed. S Braz J Chem 26:2–9

Klunk MA, Dasgupta S, Das M, Cunha MG, Wander PR (2019a) Synthesis of sodalite zeolite and adsorption study of crystal violet dye. ECS J Solid State Sci Technol 8(10):N144–N150

Klunk MA, Dasgupta S, Nunes BVG, Wander PR (2019b) Synthesis of sodalite zeolite to treatment of textile effluents. Periódico Tchê Química 16(31):778–783

Klunk MA, Dasgupta S, Schropfer SB, Nunes BVG, Wander PR (2019c) Comparative study of geochemical speciation modeling using GEODELING software. Periódico Tchê Química 16(31):816–822

Klunk MA, Shah Z, Caetano NR, Conceição RV, Wander PR, Dasgupta S, Das M (2019d) CO_2 sequestration by magnesite mineralization through interaction between Mg-brine and CO_2: integrated laboratory experiments and computerized geochemical modelling. Int J Environ Stud. https://doi.org/10.1080/00207233.2019.1675295

Klunk MA, Shah Z, Wander PR (2019e) Use of montmorillonite clay for adsorption malachite green dye. Periódico Tchê Química 16(32):279–286

Klunk MA, Das M, Dasgupta S, Impiombato AN, Caetano NC, Wander PR, Moraes CAM (2020) Comparative study using different external sources of aluminum on the zeolites synthesis from rice husk ash. Mater Res Express 7(015023):1–18. https://doi.org/10.1088/2053-1591/ab608d

Lu X, Guo Y, Xu C, Ma R, Wang X, Wang N, Zhu W (2019) Preparation of mesoporous mordenite for the hydroisomerization of n-hexane. Catal Commun 125:21–25. https://doi.org/10.1016/j.catcom.2019.03.017

Ma Z, Xie J, Zhang J, Zhang W, Zhou Y, Wang J (2016) Mordenite zeolite with ultrahigh SiO_2/Al_2O_3 ratio directly synthesized from ionic liquid-assisted dry-gel-conversion. Microporous Mesoporous Mater 224:17–25. https://doi.org/10.1016/j.micromeso.2015.11.007

Matsunaga C, Uchikoshi T, Suzuki TS, Sakka Y, Matsuda M (2012) Orientation control of mordenite zeolite in strong magnetic field. Microporous Mesoporous Mater 151:188–194. https://doi.org/10.1016/j.micromeso.2011.10.038

Meier WM, Olson DH (1992) Atlas of zeolites structure types, 3rd edn. Butterwirth-Heinemann, Oxford

Mignoni ML, Petkowicz DI, Machado NR, Pergher SBC (2007) Synthesis of mordenite using kaolin as Si an Al source. Appl Clay Sci 41(1–2):99–104. https://doi.org/10.1016/j.clay.2007.09.010

Moraes CAM, Fernandes IJ, Calheiro D, Berwanger Filho JA, Kieling AG, Rigon MR, Brehm FA, Schneider IAH, Osório E (2014) Review of the rice production cycle: by-products and the main applications focusing on rice husk combustion and

ash recycling. Waste Manag Res 32(11):1034–1048. https://doi.org/10.1177/0734242x14557379

Nishiyama N, Ueyama K, Matsukata M (1996) Synthesis of defect-free zeolite alumina composite membrane by a vapor phase transport method. Microporous Mater 7:299–308

Panda D, Kumar EA (2017) Surface modification of zeolite 4A molecular sieve by planetary ball milling. Mater Today Proc 4(2):395–404. https://doi.org/10.1016/j.matpr.2017.01.038

Radman HM, Dabbawala AA, Ismail I, Alwahedi YF, Polychronopoulou K, Vaithilingam BV, Alhassan SM (2019) Influence of salt on nanozeolite-Y particles size synthesized under organic template free condition. Microporous Mesoporous Mater. https://doi.org/10.1016/j.micromeso.2019.03.015

Santos BPS, Almeida NC, Santos IS, Marques MFV, Fernandes LD (2018) Synthesis and characterization of mesoporous mordenite zeolite using soft templates. Catal Lett 148(7):1870–1878. https://doi.org/10.1007/s10562-018-2393-5

Scapin MA (2003) Aplicação da difração e fluorescência de raios X (WDXRF): ensaios em argilominerais. Dissertação (Mestrado)—Instituto de Pesquisas Energéticas e Nucleares, São Paulo

Scott J, Guang D, Naeramitmarnsuk K, Thabuot M, Amal R (2001) Zeolite synthesis from coal fly ash for the removal of lead ions from aqueous solution. J Chem Technol Biotechnol 77:63–69. https://doi.org/10.1002/jctb.521

Shao C, Kim HY, Li X, Park SJ, Lee DR (2001) Synthesis of high-silica-content mordenite with different SiO_2/Al_2O_3 ratios by using benzene-1,2-diol as additives. Mater Lett 56(1–2):24. https://doi.org/10.1016/S0167-577X(02)00411-1

Shinzato MC, Montanheiro TJ, Janasi VA, Negri FA, Yamamoto JK, Andrade S (2008) Caracterização tecnológica das zeólitas naturais associadas às rochas eruptivas da Formação Serra Geral, na região de Piraju-Ourinhos (SP). Revista Brasileira de Geociências 38(3):525–532

Singh BK, Kim Y, Baek SB, Meena A, Sultan S, Kwak JH, Kim KS (2018) Template free facile synthesis of mesoporous mordenite for bulky molecular catalytic reactions. J Ind Eng Chem 57:363–369. https://doi.org/10.1016/j.jiec.2017.08.044

Wahono SK, Suwanto A, Prasetyo DJ, Hernawan Jatmiko TH, Vasilev K (2019) Plasma activation on natural mordenite-clinoptilolite zeolite for water vapor adsorption enhancement. Appl Surf Sci 483:940–946. https://doi.org/10.1016/j.apsusc.2019.04.033

Xianfeng L, Prins R, Bokhoven JA (2009) Synthesis and characterization of mesoporous mordenite. J Catal 262:257–265. https://doi.org/10.1016/j.jcat.2009.01.001

Zhang Y, Xu Z, Chen Q (2002) Synthesis of small crystal polycrystalline mordenite membrane. J Membr Sci 210:361–368. https://doi.org/10.1016/S0376-7388(02)00414-3

Zhang Y, Gao W, Cui L (2007) The transformation of acid leached metakaolin to zeolite beta. Stud Surf Sci Catal. https://doi.org/10.1016/s0167-2991(07)80870-6

Zhang J, Singh R, Webley PA (2008) Alkali and alkaline-earth cation exchanged chabazite zeolites for adsorption based CO_2 capture. Microporous Mesoporous Mater 111:478–487

Zhang L, Xie S, Xin W, Li X, Liu S, Xu L (2011) Crystallization and morphology of mordenite zeolite influenced by various parameters in organic-free synthesis. Mater Res Bull 46(6):894–900. https://doi.org/10.1016/j.materresbull.2011.02.018

Zhang J, Mao Y, Li J, Wang X, Xie J, Zhou Y, Wang J (2015) Ultrahigh mechanically stable hierarchical mordenite zeolite monolith: direct binder-/template-free hydrothermal synthesis. Chem Eng Sci 138:473–481. https://doi.org/10.1016/j.ces.2015.08.016

Zhou W, Zhang D-W, Bai D-S, Li S-J, Wang X-R (2015) Medium effect on dielectric relaxation behaviors of 4A zeolite bulk dispersion system. Chin Chem Lett 26(10):1255–1258. https://doi.org/10.1016/j.cclet.2015.05.046